Supporting information

Structural Defects Induced Peak Splitting in Gold-Copper Bimetallic Nanorods during Growth by Single Particle Spectroscopy

Sravan Thota[a‡], Shutang Chen[a‡], Yadong Zhou[b], Yong Zhang[c], Shengli Zou[b], and Jing Zhao[a,d]*

[a]Department of Chemistry, University of Connecticut, 55 North Eagleville Road, Storrs, Connecticut 06269-3060, United States

[b]Department of Chemistry, University of Central Florida, 4104 Libra Drive, Orlando, Florida 32816-2366, United States

[c]Centre for Material Science and Engineering, Massachusetts Institute of Technology, 77 Massachusetts Avenue, Cambridge, Massachusetts 02139, United States

[d]Institute of Materials Science, University of Connecticut, Storrs, Connecticut 06269-3136, United States

* Address Correspondence to: jing.zhao@uconn.edu

1. Large area TEM images of samples collected at different reaction times during growth process

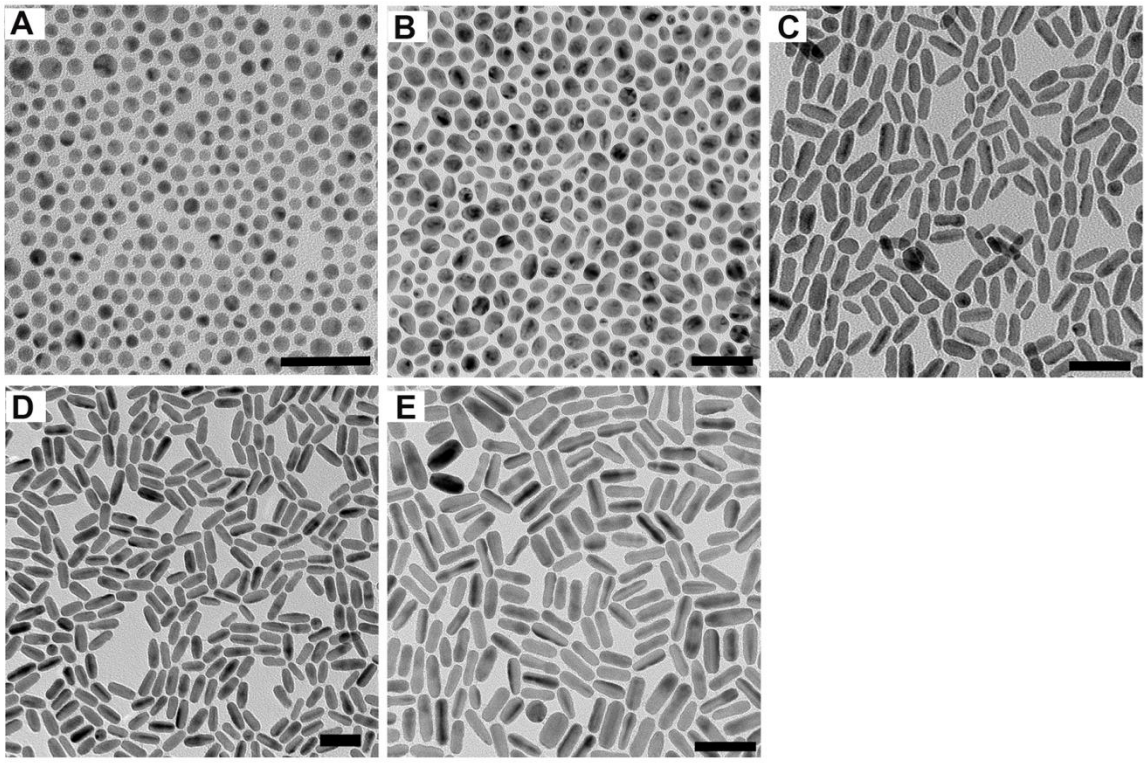

Figure S1. TEM images of the samples (A) Au seeds, and aliquots acquired at different reaction times after injection of copper precursor (B) 2 minutes (C) 5 minutes (D) 10 minutes and (E) 20 minutes. Scale bar = 50 nm.

2. Induced polarizations in a quasi-rod Au-Cu nanoparticle

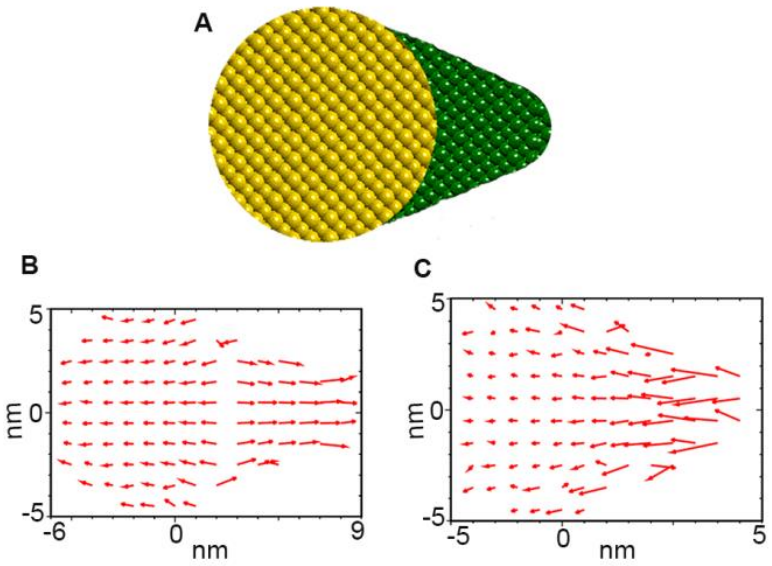

Figure S2. Induced polarizations in a quasi-rod particle. The amplitude of each vector is the modulus of the complex polarization. (A) Scheme of quasi-rod. (B) Induced polarization at 540 nm. The distribution of the polarizations shows that it is the quadrupole mode. (C) Induced polarization at 595 nm. The distribution of the polarizations shows that it is the dipole mode.

3. Scattering spectra of quasi-rod when varying the tip diameter

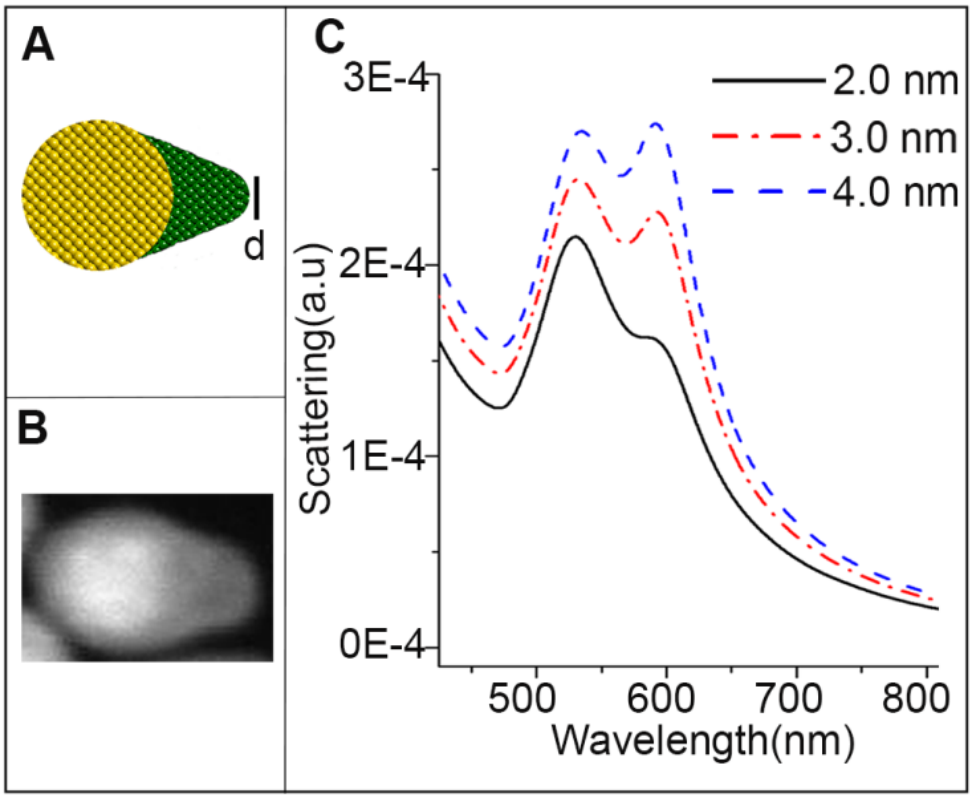

Figure S3. (A) Scheme of the quasi-rod. Yellow represents Au and green represents Cu. (B) STEM image of a representative quasi-rod particle. (C) Scattering spectra of the quasi rod when it is excited longitudinally, with tip diameters of 2 nm (black) 3nm (red) and 4 nm (blue). The Au "head" diameter is fixed at 10 nm. All the scattering spectra show two peaks at 540 nm and 595 nm.

4. Composition effect on the single particle scattering

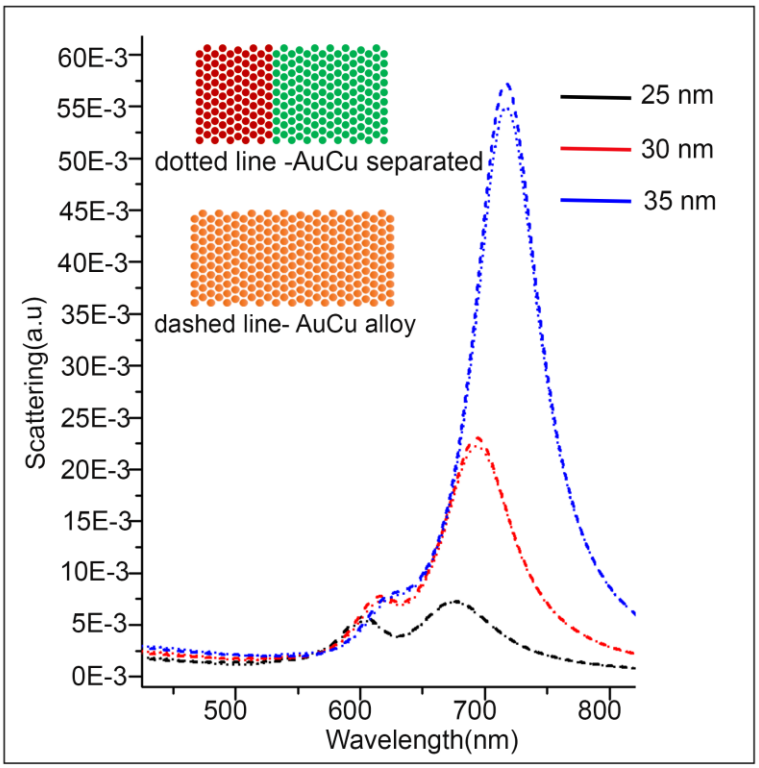

Figure S4. Schemes and calculated single particle scattering spectra of nanorods where Au and Cu were separated (dotted lines) or uniformly mixed with a 1:3 ratio (dashed lines). The lengths of the nanorods are 25 nm (black), 30 nm (red) and blue (35 nm). The calculated spectra are similar, indicating that composition has no significant effect on single particle scattering because the dielectric functions of gold and copper are similar.

5. HRTEM images of defects in rods during initial stages of growth

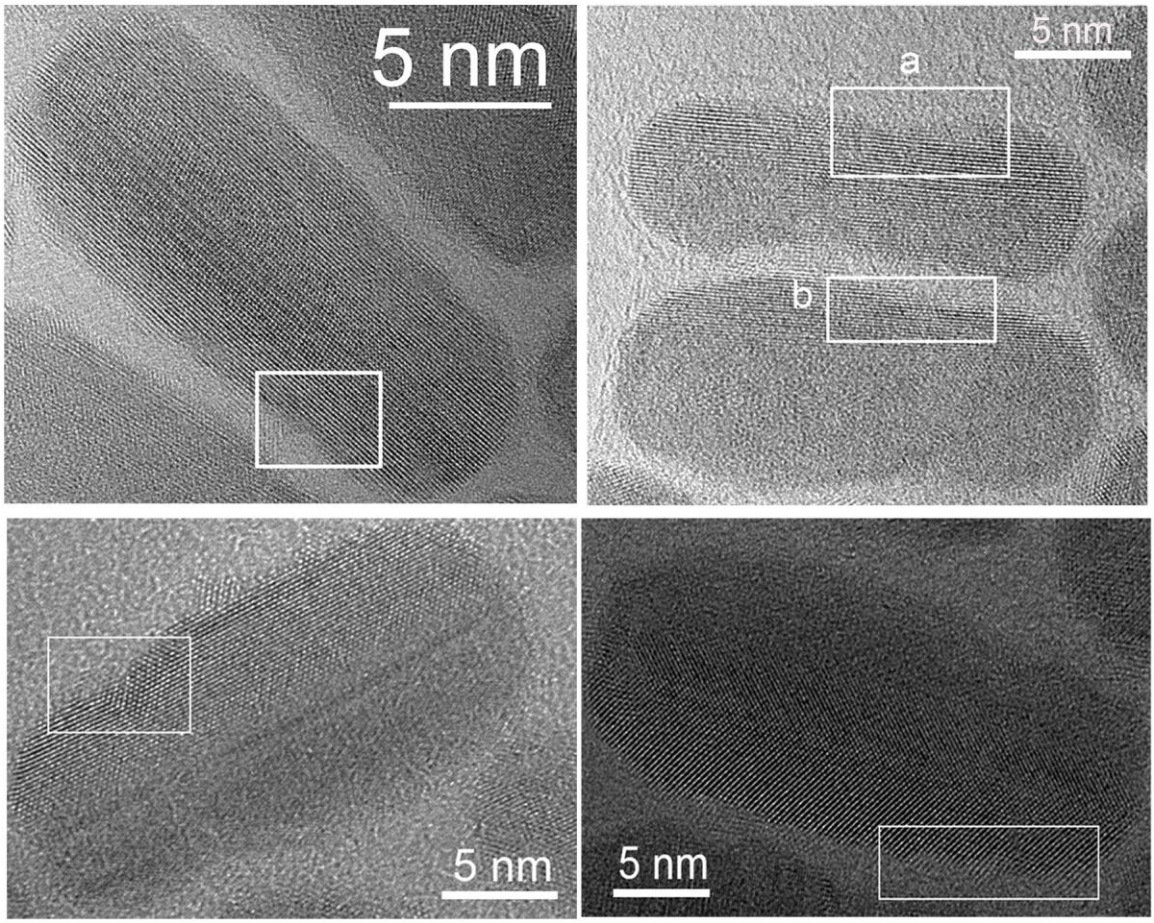

Figure S5. HRTEM images of rods with defects. Defects of different shapes and sizes are highlighted in the images. For example (a) and (b) show rods with two defects adjacent to each other and a single defect respectively.

6. Split in the longitudinal mode of an Au-Cu alloy nanorod scattering spectra caused by defect

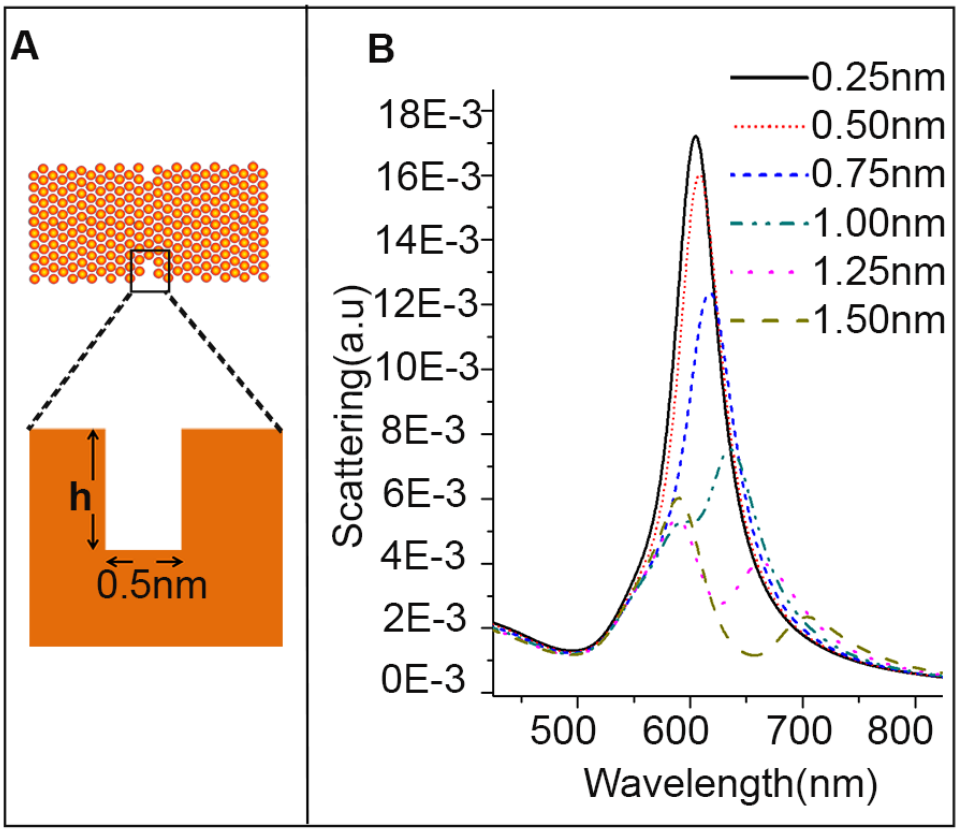

Figure S6. (A) Scheme of an Au-Cu alloy nanorod with defect. The diameter of the rod = 10 nm and the length = 20 nm. (B) Scattering spectra of the rod with defect of width 0.5 nm and varying height h = 0.25 nm (black), 0.50 nm (red), 0.75 nm (blue), 1.00 nm (sea green), 1.25 nm (pink) and 1.50 nm (light green). Defect causes the splitting in the longitudinal mode of the rod as its depth increases from 0.75 nm to 1 nm. The splitting results in two peaks, one around 600 nm and one greater than 650

7. Calucations of the induced polarizations in an Au-Cu alloy nanorod with a defect.

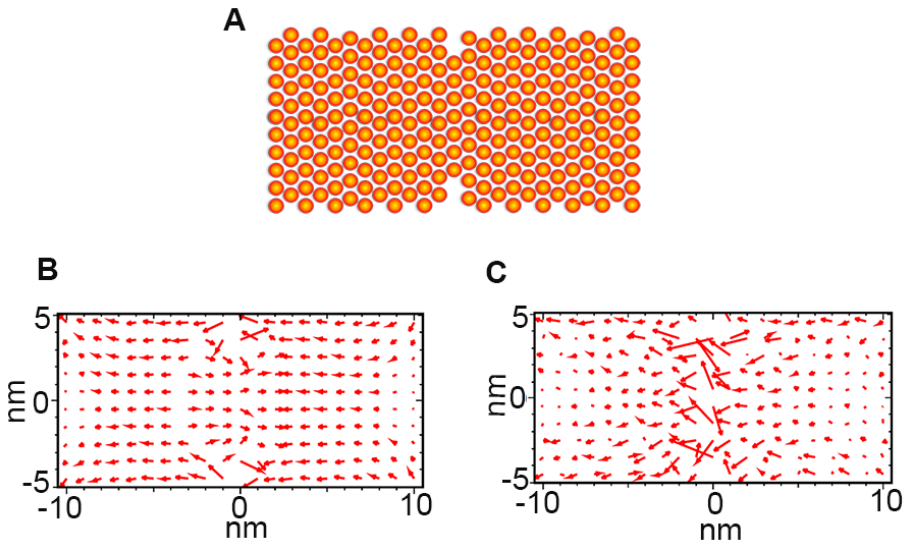

Figure S7. Induced polarizations in the Au-Cu alloy nanorod with a defect. (A) Scheme of the nanorod. The diameter of the rod = 10 nm and the length = 20 nm. The depth of the defect = 1 nm. (B) Induced polarization at 595 nm. The distribution of the polarizations shows that it is the octopole mode. (C) Induced polarization at 665 nm. The distribution of the polarizations shows that it is the dipole mode.

8. Defects coupling giving rise to new peaks in single particle scattering

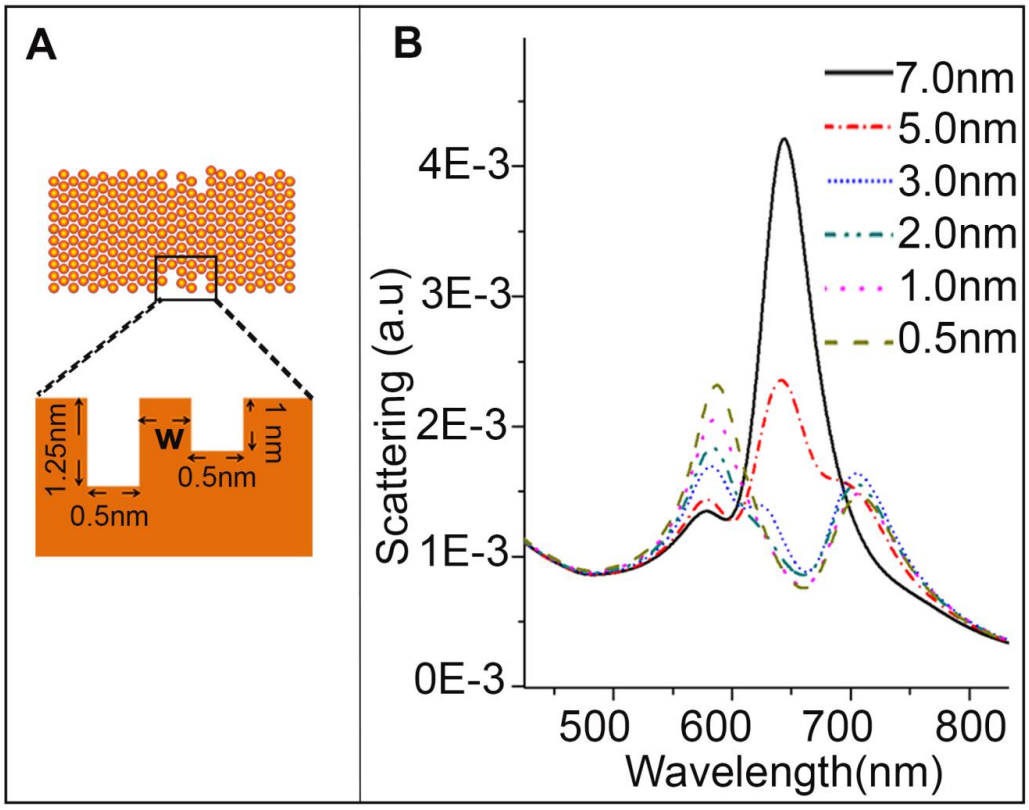

Figure S8. (A) Scheme of an Au-Cu alloy nanorod with two defects close to each other. The diameter of the rod = 10 nm and the length = 20 nm. (B) Scattering spectra of the rod with two defects of depth=1.25nm and 1nm, and width of 0.5 nm each separated by *w* = 7.0 nm (black), 5.0 nm (red), 3.0 nm (blue), 2.0 nm(sea green), 1.0 nm (pink) and 0.5 nm (light green). As *w* is reduced from 7 to 5 nm, the scattering spectrum of the rod changes from a two-peak pattern to a three-peak pattern.

9. Effect of asymmetric defects

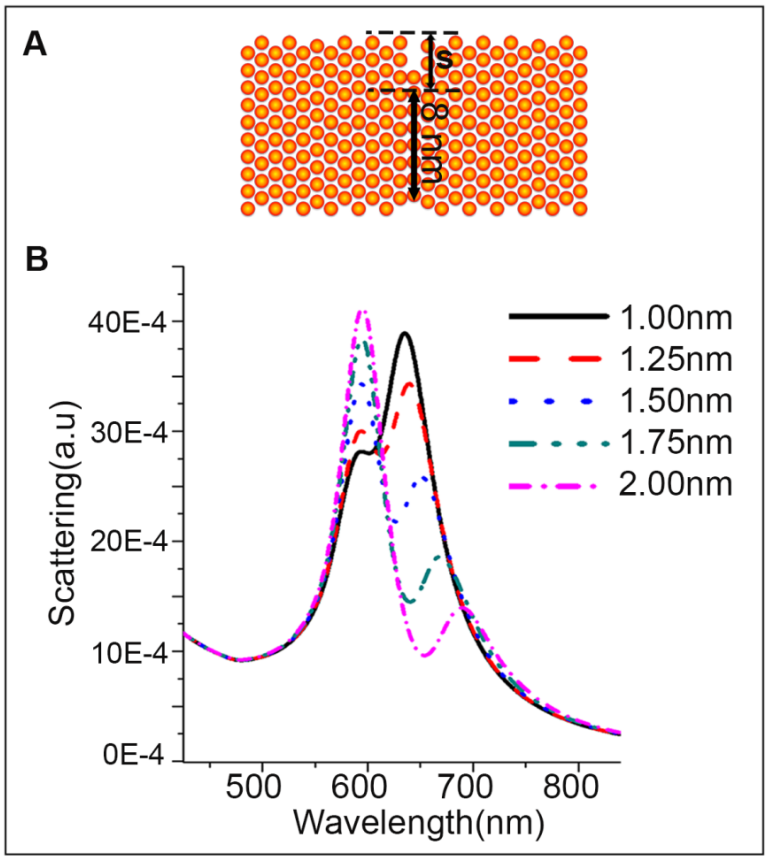

Figure S9. (A) Scheme of an Au-Cu alloy nanorod with asymmetric defects. The diameter of the rod = 10 nm and the length = 20 nm. (B) Scattering spectra of the rod obtained by shifting the central disk of width 8 nm, to one side by 0 nm (black), 0.25 nm (red), 0.50 nm (blue), 0.75 nm (sea green), and 1.00 nm (pink) between two defects of 0.5 nm width and 1.0 nm depth.

10. TEM image and single particle scattering spectra of rods obtained after 20 minutes annealing at 280° C

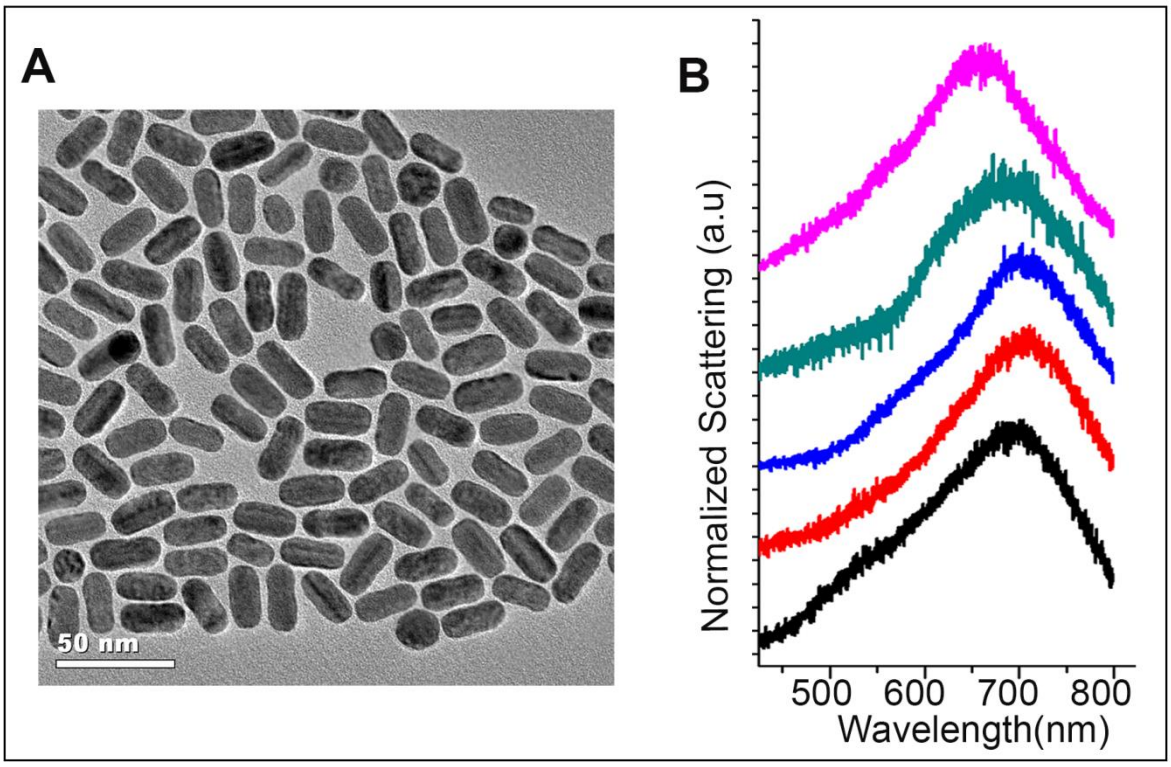

Figure S10. (A) TEM image of the annealed nanorods (B) Single nanoparticle dark field scattering spectra of the Au-Cu alloy nanorods annealed at 280° C for 20 minutes. They show only a single scattering peak from the longitudinal mode of the rod, indicating that the defects are reduced.

11. UV-VIS and XRD patterns for 20 and 30 min samples.

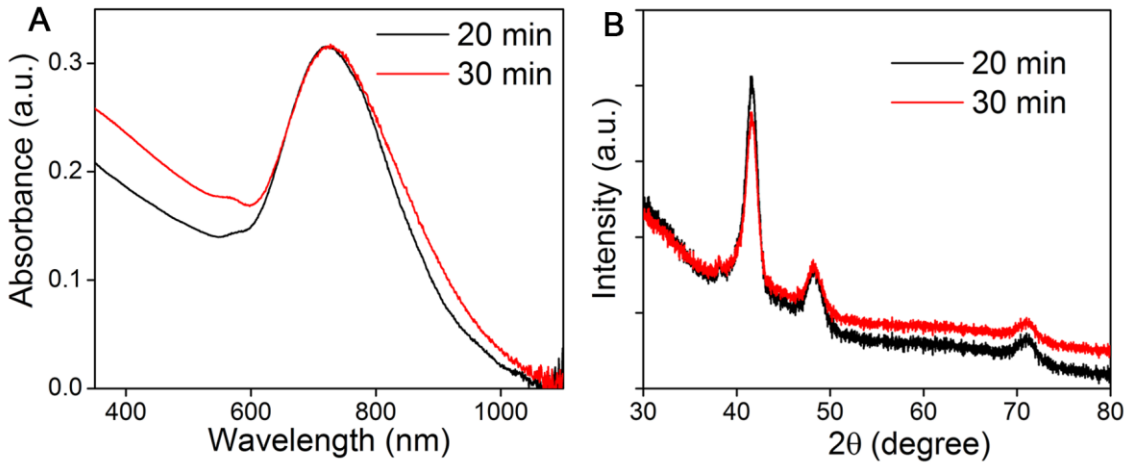

Figure S11. (A) UV-Vis-NIR spectra (B) XRD patterns of nanorod samples after 20 and 30 minutes reaction showing there is no change in the spectral patterns and reaction ended at 20 minutes.

Table S1. Population distribution of nanoparticles in different types based on peak patterns

	Single peak	Two peaks	Multiple peaks (greater than 2 peaks)
Type I	16%	-	84%
Type II	11%	-	89%
Type III	2%	-	98%
Type IV	20%	80%	-
280° C	50%	50%	-

From type I to IV, the percentage of population showing multiple peaks decrease indicating that defects are formed during the initial stage of growth as phase transition takes place. The percentage of population showing single peak increased in sample prepared at 280° C, indicating that annealing would reduce the defects and proves that defects cause multiple peak patterns in single particle dark field spectra.